Review of design codes of concrete encased steel short columns under axial compression

K.Z. Soliman, A.I. Arafa, Tamer M. Elrakib *

Housing and Building National Research Centre, Cairo, Egypt

Abstract   In recent years, the use of encased steel concrete columns has been increased significantly in medium-rise or high-rise buildings. The aim of the present investigation is to assess experimentally the current methods and codes for evaluating the ultimate load behavior of concrete encased steel short columns. The current state of design provisions for composite columns from the Egyptian codes ECP203-2007 and ECP-SC-LRFD-2012, as well as, American Institute of Steel Construction, AISC-LRFD-2010, American Concrete Institute, ACI-318-2008, and British Standard BS-5400-5 was reviewed. The axial capacity portion of both the encased steel section and the concrete section was also studied according to the previously mentioned codes. Ten encased steel concrete columns have been investigated experimentally to study the effect of concrete confinement and different types of encased steel sections. The measured axial capacity of the tested ten composite columns was compared with the values calculated by the above mentioned codes. It is concluded that non-negligible discrepancies exist between codes and the experimental results as the confinement effect was not considered in predicting both the strength and ductility of concrete. The confining effect was obviously influenced by the shape of the encased steel section. The tube-shaped steel section leads to better confinement than the SIB section. Among the used codes, the ECP-SC-LRFD-2012 led to the most conservative results.

© 2013 Housing and Building National Research Center. Production and hosting by Elsevier B.V. All rights reserved.

Introduction

For the past two decades, concrete encased steel columns are used in tall buildings. They have the rigidity and stiffness of concrete, as well as, the strength and ductility of the steel section. They also reduce the cross sectional dimensions which in turn makes them more slender and easy to erect. Composite columns can be classified as either hollow sections filled with concrete or steel sections encased in concrete. The latter one is considered in this paper. It offers high strength, ductility, fire

* Corresponding author.
E-mail addresses: k.soliman@hbrc.edu.eg (K.Z. Soliman), A.arafa@hbrc.edu.eg (A.I. Arafa), T.Rakib@hbrc.edu.eg (T.M. Elrakib).
Peer review under responsibility of Housing and Building National Research Center.

Table 1 Concrete compressive strength in the available codes.

Code	Concrete	Comment
ECP203-2007	$0.67\,f_{cu}$	Refer to 0.85×0.80 (ratio between cylinder to cube strength) = 0.68
ECP-SC-LRFD-2012	Not limited	–
ACI 318-08	$0.85\,f_{c'}$	Account for accidental eccentricities not considered in the analysis that may exist in a compression member
AISC-LRFD-2010	$0.85\,f_{c'}$	The nominal compressive strength shall be computed assuming that concrete components in compression have reached a stress of $0.85\,f_{c'}$
BS 5400-Part 5-2002	$0.67\,f_{cu}$	Refer to 0.85×0.80 (ratio between cylinder to cube strength) = 0.68

f_{cu} is the 28th day cube strength of concrete, and $f_{c'}$ is the 28th day cylinder strength of concrete.

protection for the steel section, and simplified beam to column connections. Different methods for the design of composite columns exist in codes of practice [1–5]. A composite column may be treated in some methods as a steel column strengthened by concrete. On the other hand, it may be treated as a reinforced concrete column with special reinforcement. Furthermore, the strength of a composite column may be evaluated as the sum of strengths of both components, concrete and steel reinforcements. Existing code differences may be attributed to difference in design philosophy; i.e., strain distribution and compatibility. This discrepancy is referring to the differences in allowable material properties, limiting dimensions and safety factors [6–8].

Mimoune [9] studied theoretically the monotonic behavior of composite columns under axial load and he concluded that the obtained results showed a difference between different codes of practice. It was also stated that, the confinement coefficients' values need to be adjusted.

Paul and Samanta [10] assessed the axial capacity of a concrete encased steel short column by two different codes, the Euro Code EC4 and the Load and Resistance Factor Design-American Institute of Steel Construction AISC-LFRD code using a 3D finite element model. They reported that the Euro Code EC4 method shows more accurate predictions of composite column strength. However, neither EC4 nor AISC provisions explicitly consider any increase in the strength or ductility of concrete due to transverse ties, i.e.; the confinement effect was not included so it is of importance to experimentally investigate the concrete confinement effect on the concrete encased steel composite columns.

The literature review has also indicated the scarcity of experimental data on concrete encased steel short column. Accordingly, the current research has the following goals

- Carrying out an experimental program that would lead to a better understanding of the behavior of the concrete encased steel short column.
- Analyzing the response of the tested columns in terms of strength and ductility to provide a database useful for developing design guidelines.
- Comparison between the available codes and formulas.

To achieve such goals, an experimental program comprising tests of ten encased steel composite concrete columns designated as CI to C10 was conducted. The tested parameters are concrete contribution, concrete confinement through using different stirrups ratio and also the different types of encased steel sections.

Brief description of the available design codes for composite columns

Different concepts for the design of composite columns exist in the available codes of practice [1–5], will be summarized hereinafter,

ECP 203-2007 [1]

The design of composite columns is based on the limit state design method with loading factors and partial safety for materials. The strength of a composite column is computed as for reinforced concrete members. Failure is defined in terms of a 0.002 strain limit for any concrete fiber. However, the slenderness and area parameters are modified for the presence of the steel section. Load transfer should be provided by direct bearing at the connections. The load carried by the concrete shall not exceed the allowable bearing stress to avoid overstressing of concrete.

ECP-Sc-LRFD-2012 [2]

It is based on limit state design with loading factors, partial safety for materials, modified yield stress, modified young's modulus, modified radius of gyration and numerical quantification. The design of composite columns is based on the design equations for steel columns. However, the slenderness and area parameters are modified for the presence of concrete. Load transfer should be provided by direct bearing at the connections. The load carried by the concrete shall not exceed the allowable bearing stress to avoid overstressing of concrete.

ACI-318-08 [3]

It uses the limit state design format with factors and capacity reduction factors. The strength of a composite column is computed as for reinforced concrete members. Failure is defined in terms of a 0.002 strain limit for any concrete fiber. The expression for equivalent stiffness includes a creep factor, and cracked concrete stiffness is considered. Minimum eccentricities are specified to cover construction tolerances.

AISC-LRFD-2010 [4]

The load and resistance factor design uses the limit state design method with loading factors and capacity reduction factors.

Table 2 Equivalent stiffness in the available codes.

Code	E_c	Comments
ECP203-2007	$E_c = 4400 \sqrt{f_{cu}}$ (N/mm^2)	A cracked section is used, with a creep factor
ECP-SC-LRFD-2012	22000–31000 N/mm^2 for $f_{cu} = 25$–50 N/mm^2	–
ACI-318-08	$E_c = 4700 \sqrt{f_{c'}}$ (N/mm^2)	A cracked section is used, with a creep factor
AISC-LRFD-2010	$E_c = 0.043 \, w_c^{1.5} \sqrt{f_{c'}}$ (N/mm^2)	A cracked section is used, (w_c = unit weight of concrete in kg/m^3)
BS 5400-Part 5-2002	$E_c = 670 \, f_{cu}$	A cracked section is used, with a creep factor

Table 3 Properties of the used materials in the available codes.

Code	Concrete strength	Steel yield Strength
ECP203-2007	$f_{cu} \geqslant 20$ N/mm^2	$f_y \leqslant 350$ N/mm^2
ECP-SC-LRFD-2012	25 N/mm$^2 < f_{cu} < 50$ N/mm^2	(Not limited)
ACI-318-08	$f_{c'} > 17$ N/mm^2	$f_y < 350$ N/mm^2
AISC-LRFD-2010	21 N/mm$^2 < f_{c'} < 70$ N/mm^2	$f_y < 525$ N/mm^2
BS 5400-Part 5-2002	$f_{cu} > 25$ N/mm^2	Grade 430 and 500 N/mm^2

Table 4 Steel and concrete contributions in the available codes.

Code	Specifications
ECP203-2007	$1\% \leqslant A_{\text{Longitudinal bars + steel section}} \leqslant 6\% \, A_{\text{net area of concrete}}$
ECP-SC-LRFD-2012	$A_{\text{steel section}} \geqslant 4\% \, A_{\text{gross of column}}$
ACI-318-08	$1\% \leqslant A_{\text{Longitudinal bars}} \leqslant 8\% \, A_{\text{net area of concrete}}$
AISC-LRFD-2010	$A_{\text{steel shape}}/A_{\text{gross of the member}} \geqslant 1\%$
	$A_{\text{Longitudinal bars}} \leqslant 0.4\% \, A_{\text{gross area}}$
BS 5400-Part 5-2002	$0.15 < \alpha_c < 0.80$, $\alpha_c = \frac{0.45 \times A_c \times f_{cu}}{N_u}$ where, α_c: concrete contribution

Table 5 Slenderness ranges in the available codes.

Code	Specifications
ECP203-2007	$\lambda_{\text{(slenderness ratio)}} \leqslant 50$, for braced building
	$\lambda \leqslant 35$, for unbraced building
ECP-SC-LRFD-2012	$\lambda = (L(F_{ym}/E_m)^{0.5})/\pi r_m$
	Two cases, $\lambda \leqslant 1.1$ and $\lambda \geqslant 1.1$
ACI-318-08	$\lambda = kl_{\text{(Buckling length)}}/r_{\text{(Radius of gyration for steel and concrete)}}$
AISC-LRFD-2010	Based on the ratio between the nominal compressive axial load P_{no}, and elastic critical buckling load P_e
	The available compressive strength $P_n \geqslant$ the specified for the bare steel member
BS 5400-Part 5-2002	$\frac{l_{\text{eff}}}{b} \leq 30$ short column
	$L_y/b_{\text{(breadth of column)}} \leqslant 12$, and
	$L_x/h_{\text{(depth of column section)}} \leqslant 12$

The design of composite columns is based on the design equations for steel columns. The slenderness and area parameters are modified for the presence of concrete. Load transfer should be provided by direct bearing at the connections.

BS 5400-Part 5 [5]

It is based on limit state design with loading factors and partial safety for materials. Reduced concrete properties are used to account for the effect of creep and the use of the un-cracked concrete section in stiffness calculation. The slenderness parameter is consistent with the design of steel columns as the method reduces to the bare steel column design when the concrete portion is removed.

Comparison between different codes

From above, it is obvious that there are differences between codes in design philosophy [6]. However, brief comparisons of recommended values for concrete strength, equivalent stiffness, and limits of extreme values of concrete crushing and steel yield strength, are summarized in Tables 1–3. In addition, limits of steel and concrete contribution as well as limits of
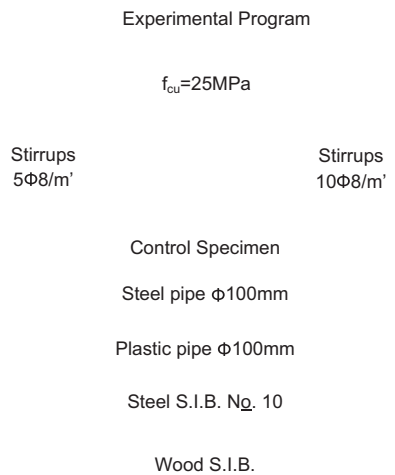
Experimental Program

f_{cu}=25MPa

Stirrups
5Φ8/m'

Stirrups
10Φ8/m'

Control Specimen

Steel pipe Φ100mm

Plastic pipe Φ100mm

Steel S.I.B. No. 10

Wood S.I.B.

Fig. 1 Experimental program.

slenderness for concrete encased columns are given in Tables 4 and 5.

Experimental test program

Characteristics of test specimens

Ten encased steel composite concrete columns were designed to investigate the effect of the tested parameters which are the concrete contribution, the concrete confinement through using different stirrups ratio, as well as, different types of encased steel sections, A_{ss}. Determination of the axial capacity portion for both the encased steel section and the concrete section is also investigated. The concrete compressive strength, f_{cu} was 25 MPa for all columns. The yielding strength, f_y, of the encased sections was 240 MPa. All columns had a square cross section of size 200×200 mm with entire height 1400 mm, and were longitudinally reinforced by 4 bars of

Table 6 Properties of the tested composite columns, $f_{cu} = 25$ MPa.

Group	Col.	Section properties				A_c (net) (mm^2)	$^b A_{ss}$ (mm^2)
		Dimension $b \times d$ (mm)	A_s^a	Stirrups	Steel Sec.		
1	C1	200×200	4T12	5R8/m′	___	40,000	___
	C2	200×200	4T12	5R8/m′	Steel pipe Ø100	37,928	1099
	C3	200×200	4T12	5R8/m′	Plastic pipe Ø100	38,606	—
	C4	200×200	4T12	5R8/m′	Steel S.I.B.10	38,488	1060
	C5	200×200	4T12	5R8/m′	Wood S.I.B	36,748	—
2	C6	200×200	4T12	10R8/m′	___	40,000	___
	C7	200×200	4T12	10R8/m′	Steel pipe Ø100	37928	1099
	C8	200×200	4T12	10R8/m′	Plastic pipe Ø100	38,606	—
	C9	200×200	4T12	10R8/m′	Steel S.I.B.10	38,488	1060
	C10	200×200	4T12	10R8/m′	Wood S.I.B	36,748	—

T denotes high grade deformed bars, and the following number indicates the diameter in mm.
R denotes mild steel, and the following number indicates the diameter in mm.
^{a} A_s is the longitudinal reinforcement.
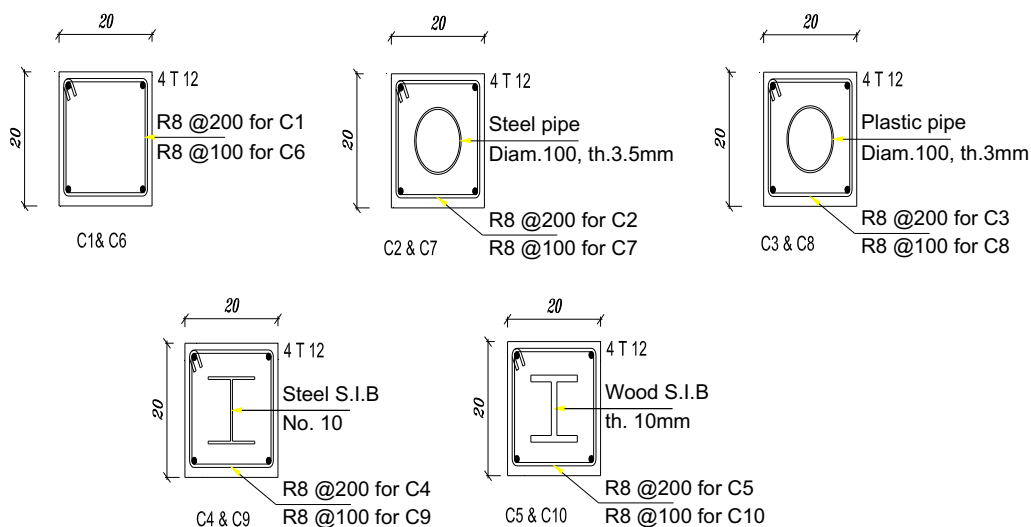^{b} A_{ss} is the area of encased steel section.

20

20

4 T 12

R8 @200 for C1
R8 @100 for C6

C1& C6

20

20

4 T 12

Steel pipe
Diam.100, th.3.5mm

R8 @200 for C2
R8 @100 for C7

C2 & C7

20

20

4 T 12

Plastic pipe
Diam.100, th.3mm

R8 @200 for C3
R8 @100 for C8

C3 & C8

20

20

4 T 12

Steel S.I.B
No. 10

R8 @200 for C4
R8 @100 for C9

C4 & C9

20

20

4 T 12

Wood S.I.B
th. 10mm

R8 @200 for C5
R8 @100 for C10

C5 & C10

Fig. 2 Details of the tested columns.

Table 7 Specimens' cube compressive strength, f_{cu}.

Specimen No.	f_{cu} (MPa)
C4, C5, C9, C10	23.1
C1, C2, C6, C7	23.7
C3, C8	22.1

12 mm diameter high-grade steel (400/600). Mild steel with $f_y = 320$ MPa was used for stirrups. The tested columns are divided into two main groups according to the spacing between stirrups, refer to Fig. 1. The first group contains columns from C1 to C5 with spacing between stirrups = 200 mm while the second group contains the columns C5 to C10 with spacing between stirrups = 100 mm. Columns, C1 and C6, are considered as control specimens without any encased steel section. Columns C2 and C7, had encased steel pipes of 100 mm diameter and 3.5 mm thickness. Columns C3 and C8, had encased plastic pipes of 100 mm diameter and 3 mm thickness. Columns C4 and C9, had encased steel Standard I Beam, S.I.B No. 10. Finally, columns C5 and C10 had encased wood Standard I Beam, of thickness 10 mm. All specimens were constructed and tested in the laboratory of the Housing and Building National Research Centre. The details of the tested specimens are illustrated in Table 6 and Fig. 2. The used concrete mix for casting all the columns was produced from ordinary Portland cement, natural sand and crushed dolomite with a maximum size of 10 mm. The columns were demolded after 24 h from casting, covered with wet burlap and stored under the laboratory conditions for 28 days before proceeding to testing stage. The quality control concrete cubes were crushed at the same time as applying the specimen's tests to determine the actual concrete compressive strength and the obtained results are shown in Table 7.

Instrumentation and testing procedure

Four linear variable differential transducers (LVDT) with stroke ± 50 mm were used to measure the columns longitudinal strains. This Pattern of gages allows for accurate axial strain measurements and traces any unintended eccentricity during loading. The gauge length was chosen equal to 1000 mm to represent the actual deformation of the column away from stress concentration zones at the upper and lower machine's heads. All transducers were mounted using pegs drilled inside the core of the columns to get the actual deformations of the concrete. In addition, electrical strain gages of 10 mm length were installed at the stirrups and middle of longitudinal reinforcement. The data were collected automatically by using a data acquisition system. Fig. 3 represents a schematic diagram of the test setup. A compression testing machine of 500 ton capacity was used for testing the columns. Prior to the test, each column was centered at the machine head and an initial load was applied to ensure concentric loading. All the columns were tested up to failure which was recognized when a sudden drop in the applied load was reached.

Experimental results

Crack pattern and mode of failure

During testing, the columns surfaces were observed in order to follow the development and the propagation of cracks. The appearance of these cracks was always a sign that the column has attained the failure state. The failure mechanisms of the tested columns with and without the encased steel section were almost the same. The damage sequence for columns was as follows: inclined cracks occurred at the upper or lower part of the column and with increasing of the applied load cracks became wider and the cover started to spall off. Finally, crushing of concrete occurred followed by buckling of vertical steel reinforcement. Fig. 4 shows the crack patterns and the mode of failure of the tested columns.

Load-vertical deformation relationship

Figs. 5–9 show the axial load versus average concrete axial deformation for all the tested columns. Also, Table 8 shows
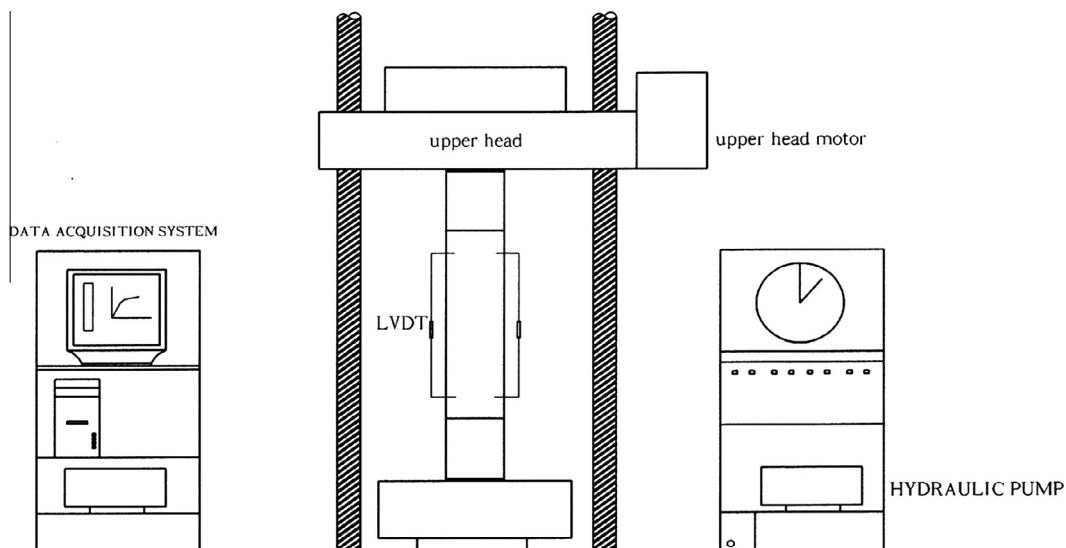
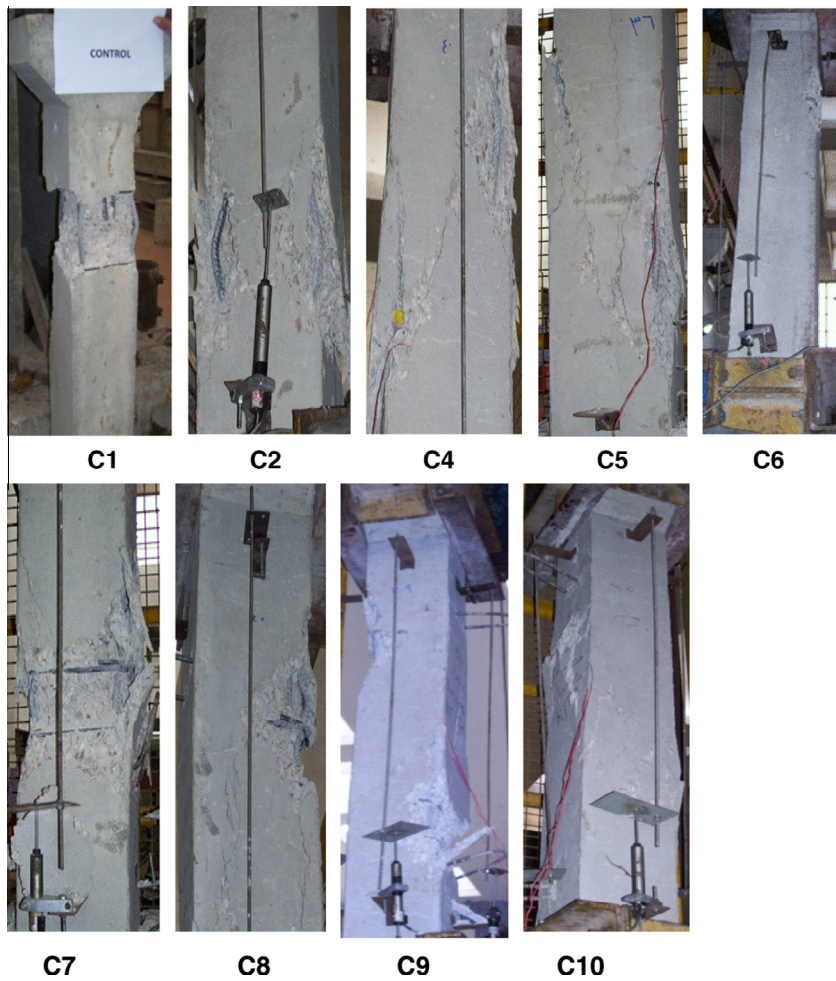**Fig. 3** Schematic diagram of the test setup for the tested columns.
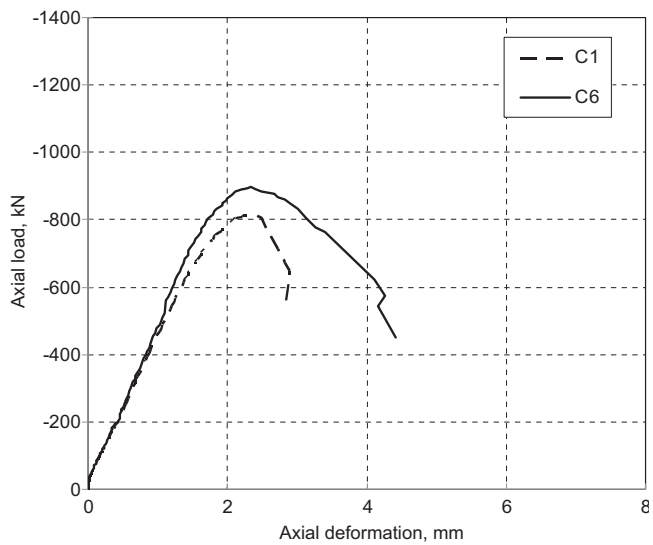
Fig. 4 Failure patterns of the tested columns.

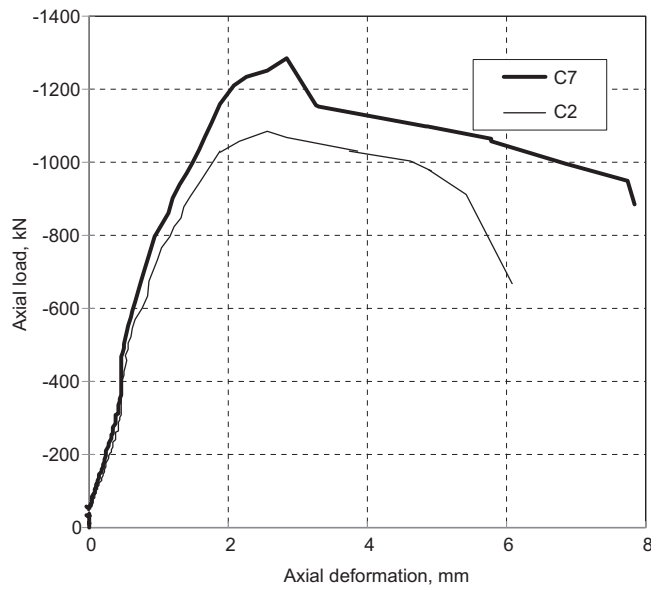**Fig. 5** Load versus vertical deformation for control columns, C1 and C6.

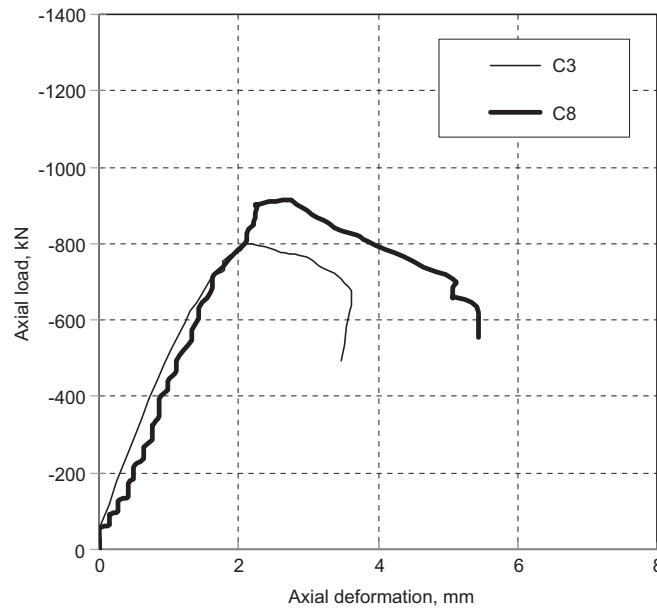**Fig. 6** Load versus vertical deformation for tested columns with steel pipe, C2 and C7.

Fig. 7   Load versus vertical deformation for tested columns with plastic pipe, C3 and C8.
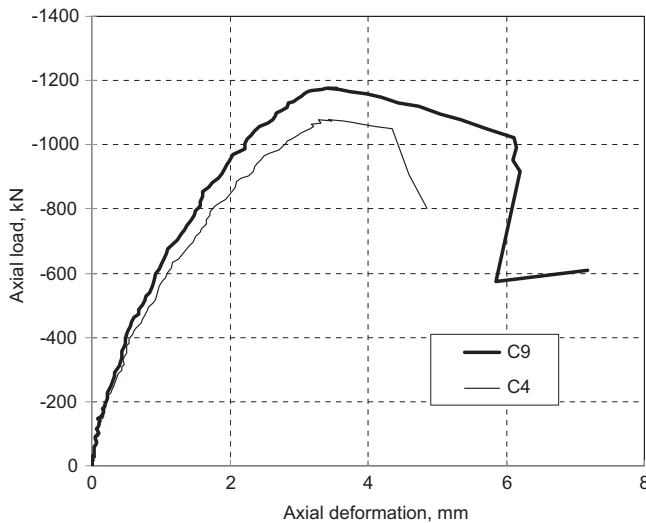

Fig. 8   Load versus vertical deformation for tested columns with steel SIB, No. 10, C4 and C9.
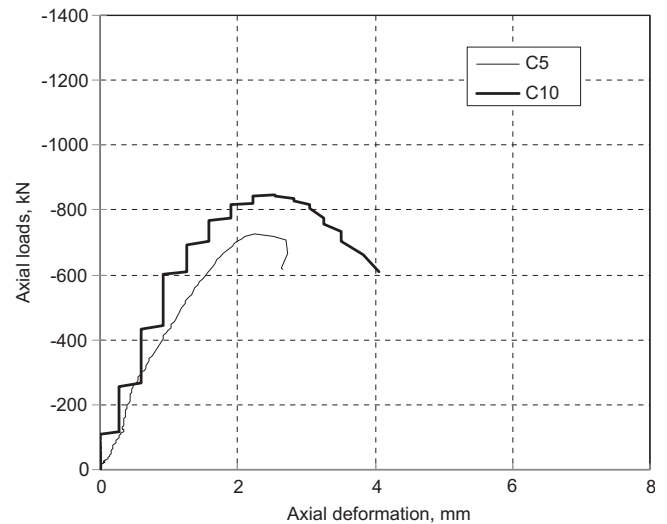

Fig. 9   Load versus vertical deformation for tested columns with wood shape SIB, C5 and C10.

the ultimate load P_u, the corresponding axial deformation Δ_u and the ductility factor μ. All the curves start with a linear part where the slope of confined concrete is close to that of unconfined concrete. At stress levels near the ultimate stress of unconfined concrete, the curves start to bend indicating that the concrete had cracked and the stirrups started their confining action. Increasing the number of stirrups from 5R8/m in the first group to 10R8/m in the second one led to increase in the column's ultimate load by 10%, 17%, 14%, 12% and 16.5% for columns C6, C7, C8, C9, and C10, respectively. Also, the ductility factor increased by 23%, 19%, 21%, 17% and 29% for the same previous columns, so it can be concluded that beyond the ultimate load, the descending branch of the load-deformation curves had a real relation with spacing of the lateral stirrups.

Columns C2 and C3 were identical in terms of concrete compressive strength, reinforcement ratio, and confinement configuration and only the presence of the encased steel section as C2 had a steel pipe and C3 had a plastic one. The ultimate load of C2 was 36% higher than that of C3 and the ductility factor of C2 was also 65% higher than that of C3. Consequently, the experimental ratio of concrete contribution was 74%. Columns C7 and C8 had the same aspects of C2 and C3, respectively except that they had double the amount of stirrups. The ultimate load of C7 was 39% higher than that of C8 leading to an experimental concrete contribution ratio of 71% while the ductility factor of C7 was 50% higher than that of C8, see Table 8.

Table 8 Experimental results of the tested columns.

Group1, Stirrups 5R8/m′					Group2, Stirrups 10R8/m′				
Col. No.	P_u (kN)	Δ_u (mm)	Δ_f^a (mm)	Δ_y^b (mm)	μ^c	Col. No.	P_u (kN)	Δ_u (mm)	Δ_f^a (mm)	Δ_y^b (mm)	μ^c
C1	815	2.35	2.87	1.38	2.1	C6	895	2.48	3.74	1.42	2.6
C2	1080	2.56	5.81	1.35	4.3	C7	1273	2.84	7.45	1.45	5.2
C3	794	2.27	3.45	1.28	2.6	C8	910	2.64	5.28	1.63	3.2
C4	1050	3.08	4.85	1.70	2.9	C9	1170	3.21	6.35	1.85	3.4
C5	726	2.56	2.57	1.35	1.91	C10	854	2.24	3.23	1.31	2.42

[a] Δ_f is the deformation corresponding to a load equal to 75% of the ultimate load on the descending branch of the load-deformation curve.
[b] Δ_y is the deformation corresponding to the intersection of the secant stiffness at a load equal to 75% of the ultimate load and the tangent at the ultimate load.
[c] μ is the ductility factor = (Δ_f/Δ_u).

Columns C4 and C5 were identical in all aspects except for the presence of an encased steel section as C4 had a steel S.I.B. 10 and C5 had a wooden one. The ultimate load of C5 was 44% lower than that of C4 and the ductility factor of C5 was also 51% lower than that of C4 and so, the experimental ratio of concrete contribution was 69%. For columns C9 and C10 which had the same terms of C4 and C5, respectively except that they had double the amount of stirrups, the ultimate load of C9 was 37% higher than that of C10 leading to an experimental concrete contribution ratio of 72% while the ductility factor of C9 was 40% higher than that of C8.

The effect of the encased steel shape can be discussed by comparing the behavior of columns C7 and C9 which are identical in all terms except for the shape of the encased steel section. The ultimate load of C7 was 8.9% higher than that of C9 and the ductility factor of C7 was also 53% higher than that of C9. However, Column C7, with a steel pipe, significantly showed an improved descending branch and achieved the highest ductility factor, $\mu = 5.2$, which indicates the superior effect of the tube-shaped steel section in comparison with the SIB shape in C9, see Table 8. Based on all the previous measurements, it is obvious that the ultimate load and corresponding axial deformation of the tested columns varied depending on both the configuration of the lateral steel reinforcement and the encased steel shape which are not considered in the available design codes.

Strains in steel reinforcement

The strains in vertical reinforcement of the tested specimens reached yielding at the ultimate load. In addition, the recorded strains in stirrups close to the failure zone in columns C4 and C7 exceeded the yield strain. Unfortunately, in the other tested columns the available strain results did not confirm yielding of stirrups. However the observations at failure showed that the yielding of stirrups might have occurred. Sample of the measured steel strain is shown in Fig. 10.

Theoretical evaluation of the experimental results

This paper investigates and evaluates the ultimate axial compression strength of the concrete encased steel columns and also the concrete contribution to the ultimate axial load according to the available different codes. Therefore, the
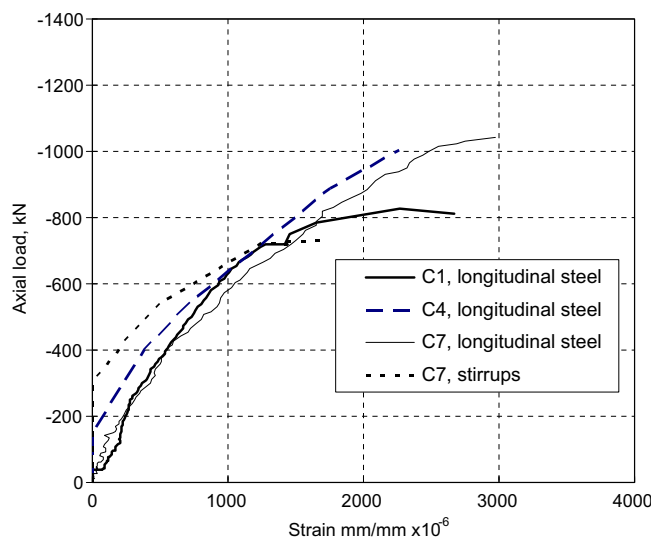

Fig. 10 Load versus steel strain for tested columns C1, C4 and C7.

encased steel sections were replaced with plastic pipes and wood shape S.I.B, instead of steel pipes and steel S.I.B sections. For each specimen, the loads carried by the concrete portion, steel portion, and the composite section were determined according to the available different codes [1–5] requirements. All the partial factors of safety for materials and the resistance factors are set to unity. This will give an unbiased comparison of the capacities predicted by the five methods since each method has its own resistance factors which are used with the corresponding load factors. The calculated capacities are presented in Table 9 and compared to the experimental results as shown in Tables 10. Among the used codes, the formulas of ECP-SC-LRFD-2012 [2] could not be applied to calculate the axial capacity of the concrete columns with no encased steel sections C1, C3, C5, C6, C8, and C10. The main equations used in the analysis are mentioned below for each code:

ECP203-2007 [1]

$$P_u = 0.35 f_{cu} A_c + 0.67 f_{ysc} A_{sc} \quad \text{(Concrete portion)}$$

Table 9 Calculated axial capacities of the tested columns according to available codes $P_{calc.}$, kN.

Column No.	Encased section		ECP203-2007 [1]	ECP-SC-LRFD -2012 [2]	ACI-318 [3]	AISC-LRFD-2010 [4]	BS-5400-5 [5]
C1,C6	Control columns	Concrete contribution	867	—	754	768	735
		Composite section	——	——	——	——	——
C2,C7	Columns with steel pipe	Concrete contribution	831	——	731	744	706
		Composite section	1208	864	1108	1063	1083
C3,C8	Columns with plastic pipe	Concrete contribution	842	——	740	754	715
		Composite section	——	——	—	——	——
C4,C9	Columns with steel SIB, No. 10	Concrete contribution	738	——	738	752	713
		Composite section	1097	785	995	928	970
C5,C10	Columns with wood shape SIB	Concrete contribution	827	—	728	740	703
		Composite section	——	——	——	——	——

Table 10a Comparison between calculated axial capacities of the tested columns and experimental results of group 1, $(P_u/P_{calc.})$.

Column No.	ECP203-2007 [1]	ECP-SC-LRFD-2012 [2]	ACI-318 [3]	AISC-LRFD-2010 [4]	BS-5400-5 [5]
C1	0.937	—	1.076	1.057	1.105
C2	0.894	1.25	0.975	1.016	0.997
C3	0.943	—	1.072	1.054	1.111
C4	0.957	1.33	1.055	1.131	1.083
C5	0.878	——	0.998	0.981	1.033
Aver.	0.94	1.29	1.04	1.05	1.06

Table 10b Comparison between calculated axial capacities of the tested columns and experimental results of group 2, $(P_u/P_{calc.})$.

Column No.	ECP203-2007 [1]	ECP-SC-LRFD -2012 [2]	ACI-318 [3]	AISC-LRFD-2010 [4]	BS-5400-5 [5]
C6	1.032	——	1.186	1.165	1.218
C7	1.054	1.47	1.149	1.197	1.176
C8	1.080	——	1.229	1.208	1.273
C9	1.067	1.49	1.176	1.260	1.207
C10	1.032	——	1.174	1.153	1.215
Aver.	1.06	1.48	1.18	1.19	1.22

Table 11 Concrete contribution ratio due to the experimental results and available codes.

Column No.	Exp. data	ECP203-2007 [1]	ACI-318 [3]	AISC-2010 [4]	BS-5400-5 [5]
C2	0.74	0.69	0.66	0.70	0.65
C4	0.69	0.75	0.74	0.80	0.73
C7	0.71	0.69	0.66	0.70	0.65
C9	0.72	0.75	0.74	0.80	0.73

$$P_u = 0.35 f_{cu} A_c + 0.67 f_{yss} A_{ss} + 0.67 f_{ysc} A_{sc} \quad \text{(Composite section)}$$

ECP-SC-LRFD-2012 [2]

$$P_u = 0.80 A_s F_{cr} \quad \text{(Composite section)}$$

$$F_{cr} = 0.648 F_{ym}/\lambda^2 \quad \text{for } \lambda \geq 1.1$$

$$F_{cr} = (1 - 0.348\lambda^2) F_{ym} \quad \text{for } \lambda \leq 1.1, \text{ where } \lambda$$
$$= \text{slenderness ratio}$$

$$F_{ym} = F_y + 0.7 F_{yr}\left(\frac{A_r}{A_s}\right) + 0.48 f_{cu}\left(\frac{A_c}{A_s}\right)$$

ACI-318-05 [3]

$$P_{n,max} = 0.80[0.85 f_{c'}(A_g - A_{st}) + f_y A_{st}] \quad \text{(Concrete portion)}$$

$$P_{n,max} = 0.85[0.85 f_{c'}(A_g - A_{st}) + f_{yss} A_{ss} + f_y A_{st}]$$
$$\times \text{(Composite section)}$$

AISC-LRFD-2010 [4]

$$P_{no} = [0.85f_{c'}A_c + f_yA_s + F_{ysr}A_{sr}] \quad \text{(Composite section)}$$

$$P_e = \pi^2(EI_{eff})/(KL)^2$$

$$P_n = 0.75 \times P_{no} \times \left[0.658^{\frac{P_{no}}{P_e}}\right], \quad \text{if } \frac{P_{no}}{P_e} \leq 2.25$$

BS 5400-Part 5 [5]

$$\alpha_c = \frac{0.45 \times A_c \times f_{cu}}{N_u} \quad \text{(Concrete contribution ratio)}$$

$$N_u = 0.91A_sf_y + 0.87A_rf_{ry} + 0.45A_cf_{cu} \quad \text{(Short column)}$$

$$N_{ay} = 0.85K_{1y}N_u \quad \text{if } \alpha_c \text{ is not applicable} \quad \text{(Composite column)}$$

Referring to Table 9, it is noticed that the calculated axial capacities of the first and second group are the same as the used codes and do not consider the confinement effect for predicting the ultimate axial strength of the columns. Referring to Table 10, the comparitive studies with the experimental results show that the predicted results are generally lower than the test results which means that the calculated column strengths using the five previous codes are almost on the conservative side. For group 1, ACI-318 [3] gives the closest prediction with an average of 4% lower than the test results and ECP-SC-LRFD-2012 [2] gives the most conservative results with an average of 29% lower than the test results. For group 2, ECP203-2007 [1] gives the closest prediction with an average of 6% lower than the test results and ECP-SC-LRFD-2012 [2] gives the most conservative values with an average of 48% lower than the test results. It is clear that considerable discrepancies exist between codes and the experimental data especially for group 2 which has excess stirrups due to neglecting of the stirrups confinement and the encased steel shape in these codes. On the other hand, the calculated ratios of concrete contribution ranged between 0.66 and 0.80 according to codes [1,3–5], and it varied from 0.69 to 0.74 according to experimental results, see Table 11.

Conclusions

Within the present scope of work and investigation carried out, the following conclusions may be drawn:

1. A non-negligible difference between the available codes of practice and the experimental results is shown. The introduction of confinement coefficients has a great influence on the ultimate calculated axial loads.

2. The values of confinement coefficients need to be adjusted in the used codes as they neglect the increase in strength and ductility of columns due to transverse ties.
3. The confining effect is obviously influenced by the shape of the encased steel section. The tube-shaped steel section led to better confinement than the SIB section which resulted in a noticeable increase in both ductility and ultimate axial capacity of the columns.
4. The calculated column strengths using the five previous codes are found to be mostly conservative when compared with the experimentally obtained test results. However, the ECP-SC-LRFD-2012 formula led to the most conservative results.
5. Finally, the concrete contribution is mainly dependent on the number of ties and shear transfer between the concrete and steel sections. Despite this, no specific requirements for calculating shear transfer between the encased steel section and concrete are available in the design codes. Future researches are needed to cover this point.

References

[1] Egyptian Code of Practice for Design and Construction of Concrete Structures, ECP 203, Housing and Building National Research Center, 2007.
[2] Egyptian Code of Practice for Steel Construction (ECP-SC-LRFD), Housing and Building National Research Center, 2012.
[3] Building Code Requirements for Reinforced Concrete, American Concrete Institute, ACI 318, Detroit, 2008.
[4] Specification for Structural Steel Buildings, (AISC-LRFD), American Institute of Steel Construction, Chicago, Illinois, 2010.
[5] Steel, Concrete and Composite Bridges, Part 5, (BS.5400-5): Code of Practice for Design of Composite Bridges, 2002.
[6] S. El-Tawil, G. Gregory, Strength and ductility of concrete encased composite columns, J. Struct. Eng. 125 (1999) 1009–1019.
[7] C. Weng, S. Yen, Comparisons of concrete-encased composite column strength provisions of ACI code and AISC specification, Eng. Struct. 24 (2002) 59–72.
[8] N. Shanmugam, B. Lakshmi, State of the art report on steel–concrete composite columns, J. Constr. Steel Res. 57 (2001) 1041–1080.
[9] M. Mimoune, Design of Steel Concrete Composite Columns Subject to Axial Compression, Constantine University Algeria 35 (2010) 201–207.
[10] A. Paul, A. Samanta, Review of design practice of concrete encased steel short column under axial load, Int. J. Earth Sci. Eng. 4 (2011) 608–611.